

**Interseismic quiescence and triggered slip of active normal faults of Kīlauea Volcano's south flank during 2001-2018**

K. Wang<sup>\*1</sup>, H. S. MacArthur<sup>2</sup>, I. Johanson<sup>3</sup>, E.K. Montgomery-Brown<sup>4</sup>, M. P. Poland<sup>5</sup>, E. C. Cannon<sup>6</sup>, M. d'Alessio<sup>7</sup>, & R. Bürgmann<sup>1</sup>

<sup>1</sup>University of California, Berkeley, Department of Earth and Planetary Sciences, Berkeley, CA 94720, USA

<sup>2</sup>California Institute of Technology, Seismological Laboratory, Pasadena, CA 91125, USA

<sup>3</sup>United States Geological Survey, Hawaiian Volcano Observatory, Hawaii National Park, HI 96718, USA

<sup>4</sup>United States Geological Survey, California Volcano Observatory, Menlo Park, CA 94025, USA

<sup>5</sup>United States Geological Survey, Cascades Volcano Observatory, Vancouver, WA 98683, USA

<sup>6</sup>Golder Associates Inc. 2121 Abbott Road, Suite 100. Anchorage, AK 99507, USA

<sup>7</sup>California State University Northridge, Department of Geological Sciences Northridge, CA 91330, USA

**Contents of this file**

Figures S1 to S7  
Table S1 and S2

## Introduction

This file contains 7 figures (Figure S1 to S7) showing InSAR baselines and LOS offsets across the HFS and KFS, modeling effort of the newly formed fault scarp near the eastern end of the HFS, and two tables (Table S1 to S2) of interseismic GPS velocities across the HFS.

Figure S1: Baseline distribution of the SAR images used in this study

Figure S2-S3: Interferometric phase of CSK data around the Koa'e fault system

Figure S4: Interferometric phase of CSK data at the Poliokeawe and Hōlei palis of the HFS.

Figure S5: Interferometric phase of CSK data around the Pulama segment at the eastern end of the HFS.

Figure S6: LOS displacements across the Koa'e fault system derived from Sentinel-1 data.

Figure S7: Comparison of observed and modeled coseismic LOS displacements due to the newly formed costal slump near the eastern end of the HFS.

Table S1. GPS velocity across the HFS during 2001 and 2010.

Table S2. GPS velocity across the HFS during 2010 and 2017.

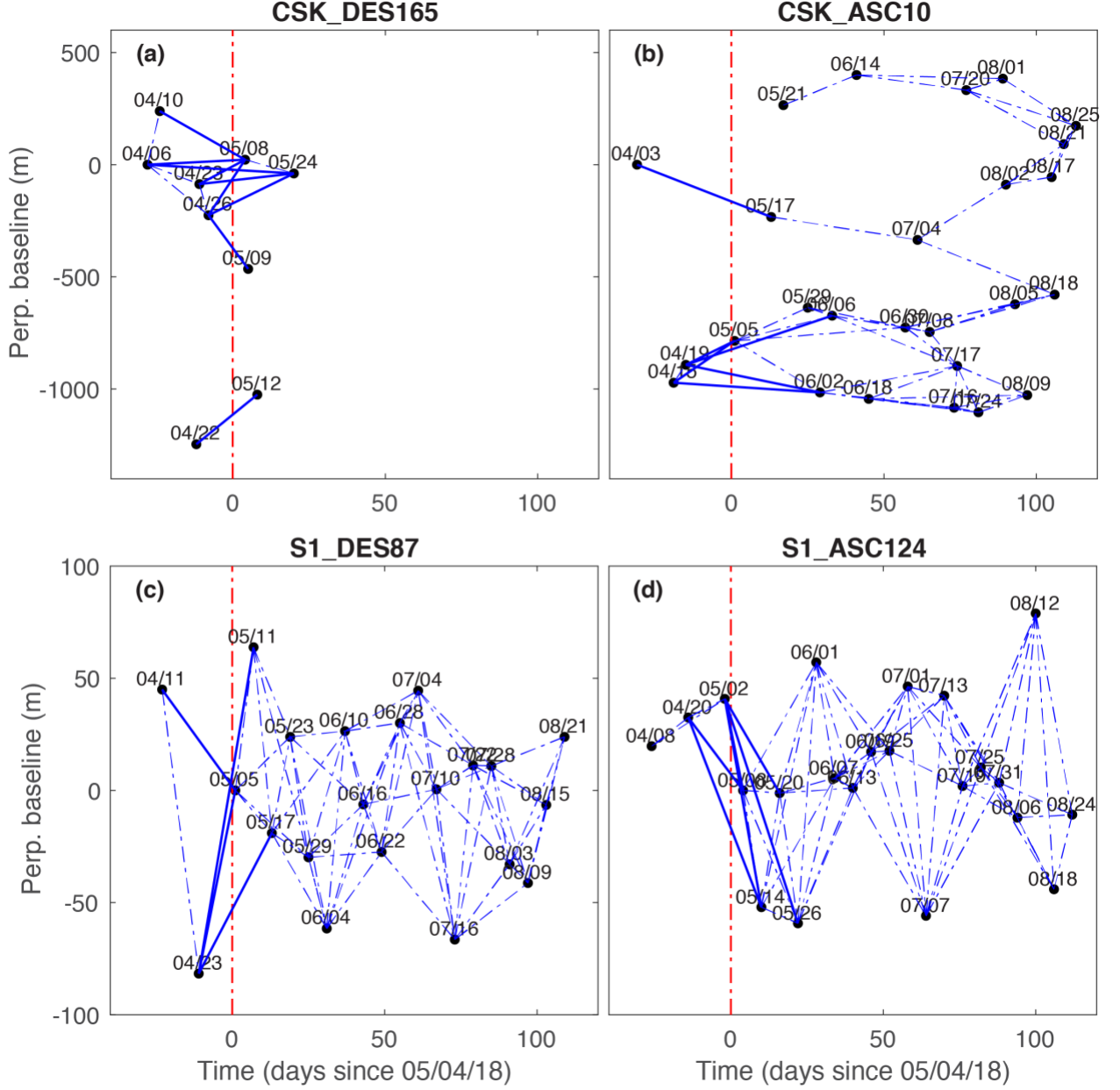


Figure S1. Baseline distribution of the SAR images for (a) COSMO-SkyMed (CSK) descending track D165, (b) CSK ascending track A10, (c) S1 descending track D87 and (d) S1 ascending track A124. Red dash-dot line represents the time of the May 4, 2018, M 6.9 earthquake on 05/04/2018. Solid blue lines denote the earthquake-spanning interferograms used to examine the coseismic offsets across the KFS and HFS. Dashed blue lines represent either pre- or post-earthquake interferograms satisfying the baseline criterias ( $B_p < 250$  m and  $B_t < 30$  days for S1 and  $B_t < 60$  days for CSK).

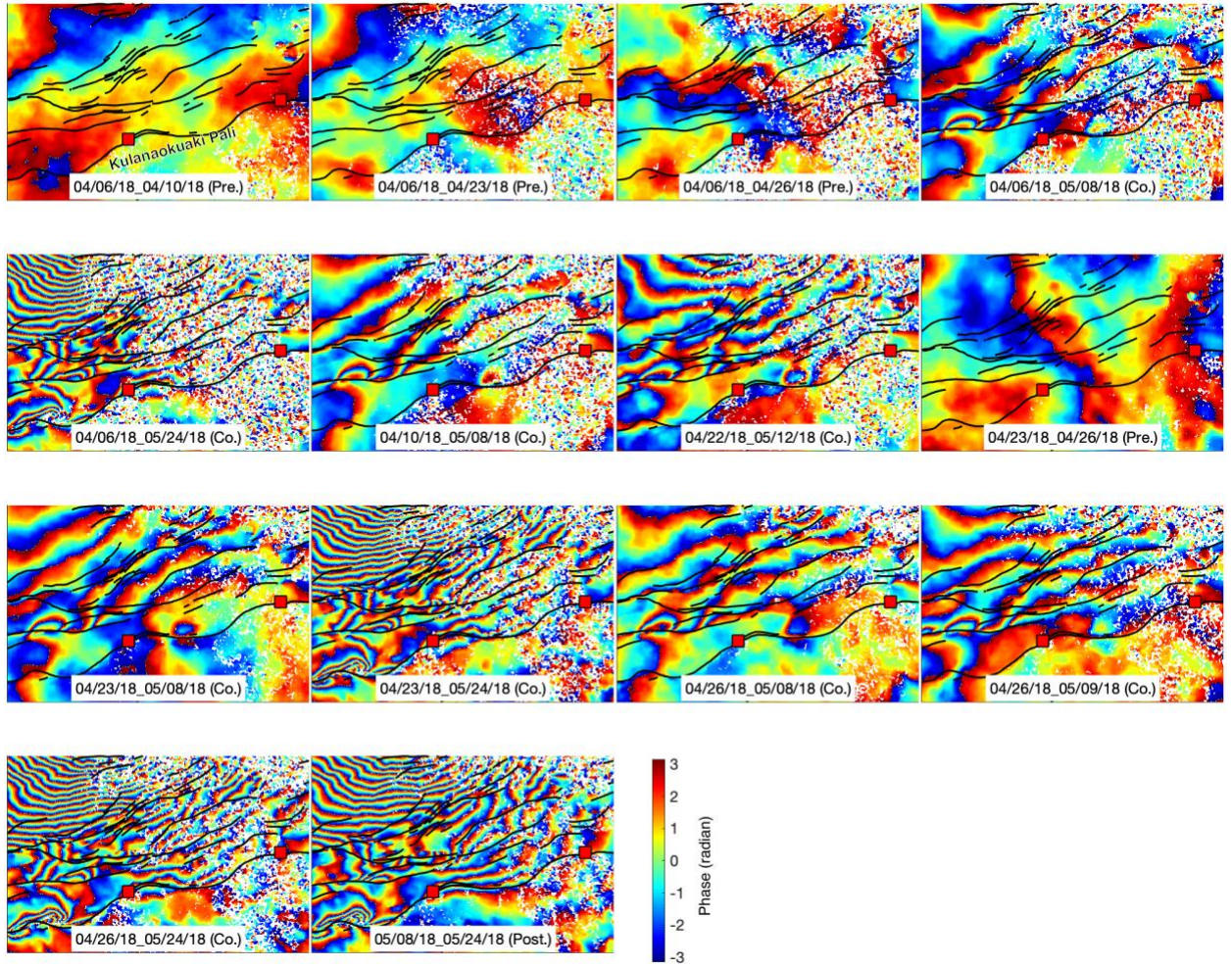


Figure S2. Interferometric phase of CSK data from the descending track D165 around the Koa'e fault system. Black lines denote previously mapped faults. Numbers in each panel represent the time of the master and slave image acquisitions. Red squares represent the locations of two field observations along the Kulanaokuaki Pali (Swanson, written comm., 2019). For all the wrapped CSK interferograms, each fringe cycle corresponds to 1.55 cm LOS displacement.



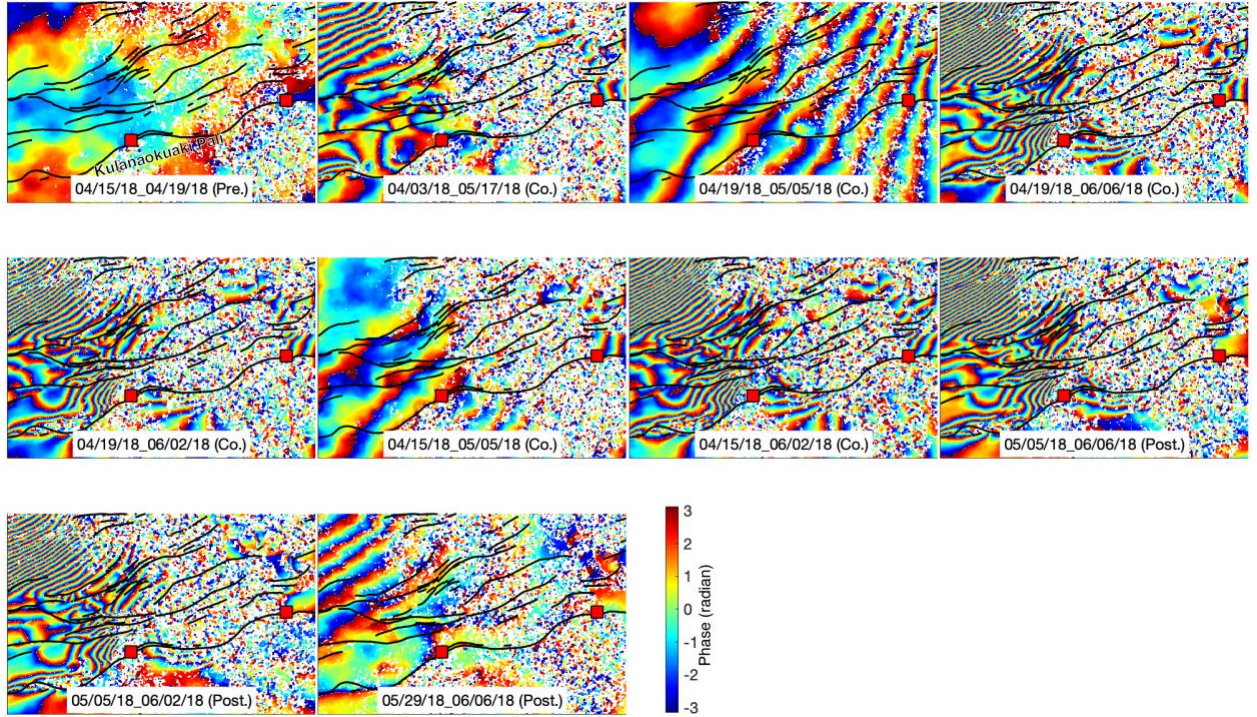


Figure S3. Interferometric phase of CSK data from the ascending track A10 around the Koa'e fault system. Black lines denote previously mapped faults. Numbers in each panel represent the time of the master and slave image acquisitions. Red squares represent the locations of two field observations along the Kulanaokuaki Pali (Swanson, written comm., 2019). Note that the interferograms with the second image acquired on 05/05/2018 do not show clear offsets across the KFS, indicating that the KFS offsets are not directly associated to the M 6.9 earthquake on 05/04/2018.

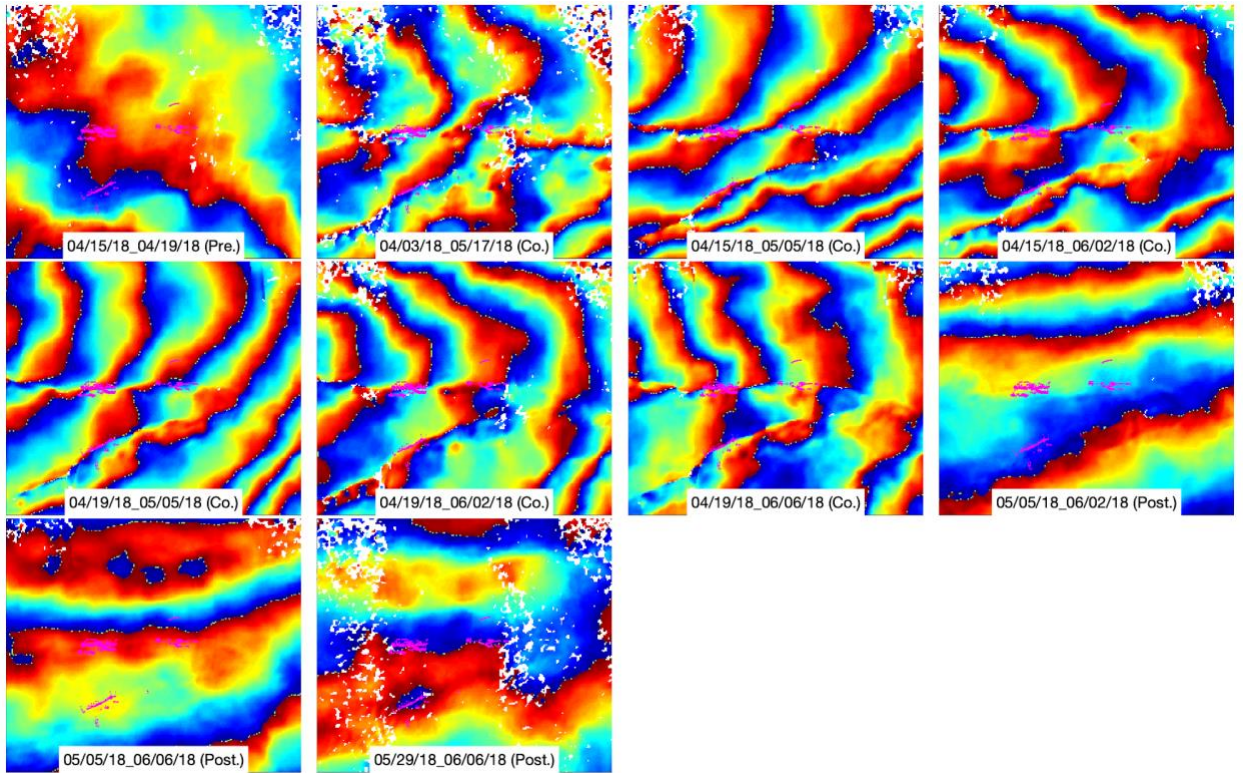


Figure S4. Interferometric phase of CSK data from the ascending track A10 at the Poliokeawe and Hōlei palis of the HFS. Magenta lines indicate mapped locations of observed offsets triggered by the 1975 M7.7 Kalapana earthquake that were mapped in fresh 1974 Mauna Ulu lava flows (Cannon and Bürgmann, 2001). Note that only interferograms spanning the M 6.9 earthquake on 05/04/2018 show the offsets across the palis.



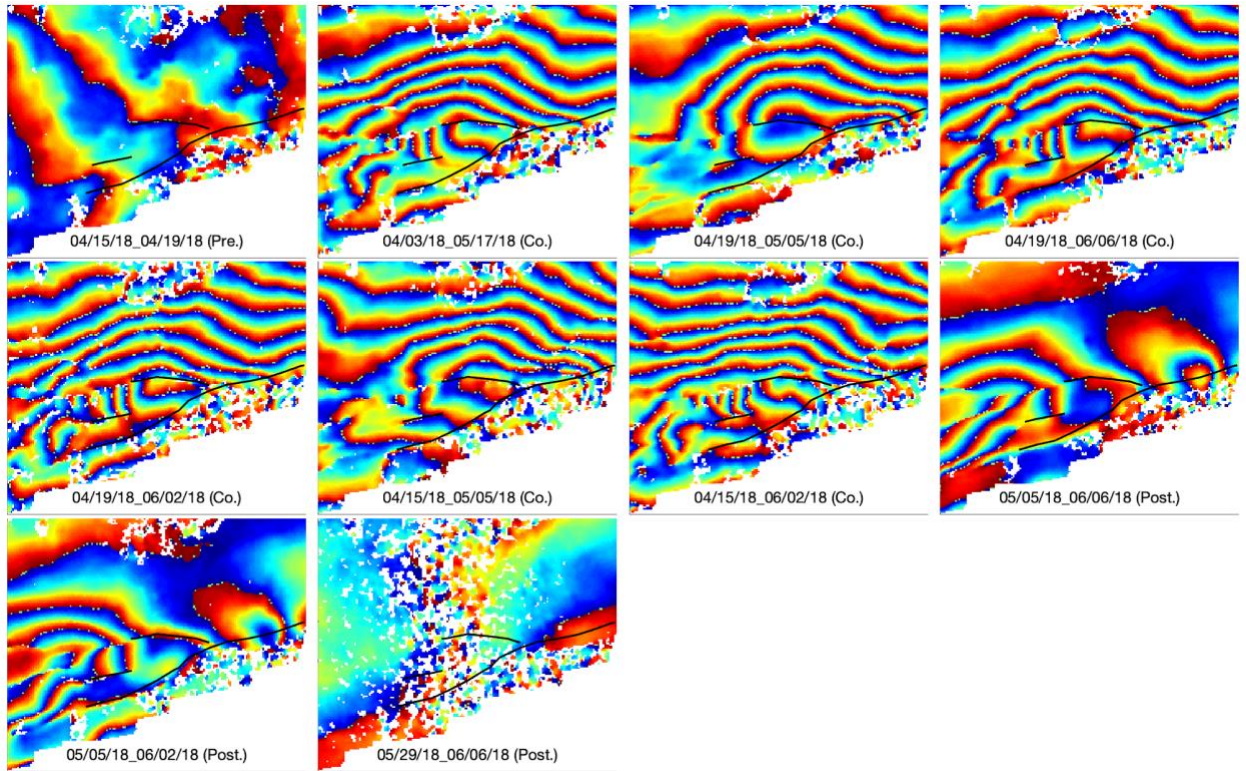


Figure S5. Interferometric phase of CSK data from the ascending track A10 around the Pulama segment at the eastern end of the HFS. Black lines denote previously mapped faults. Labels in each panel provide the time of the master and slave image acquisitions.

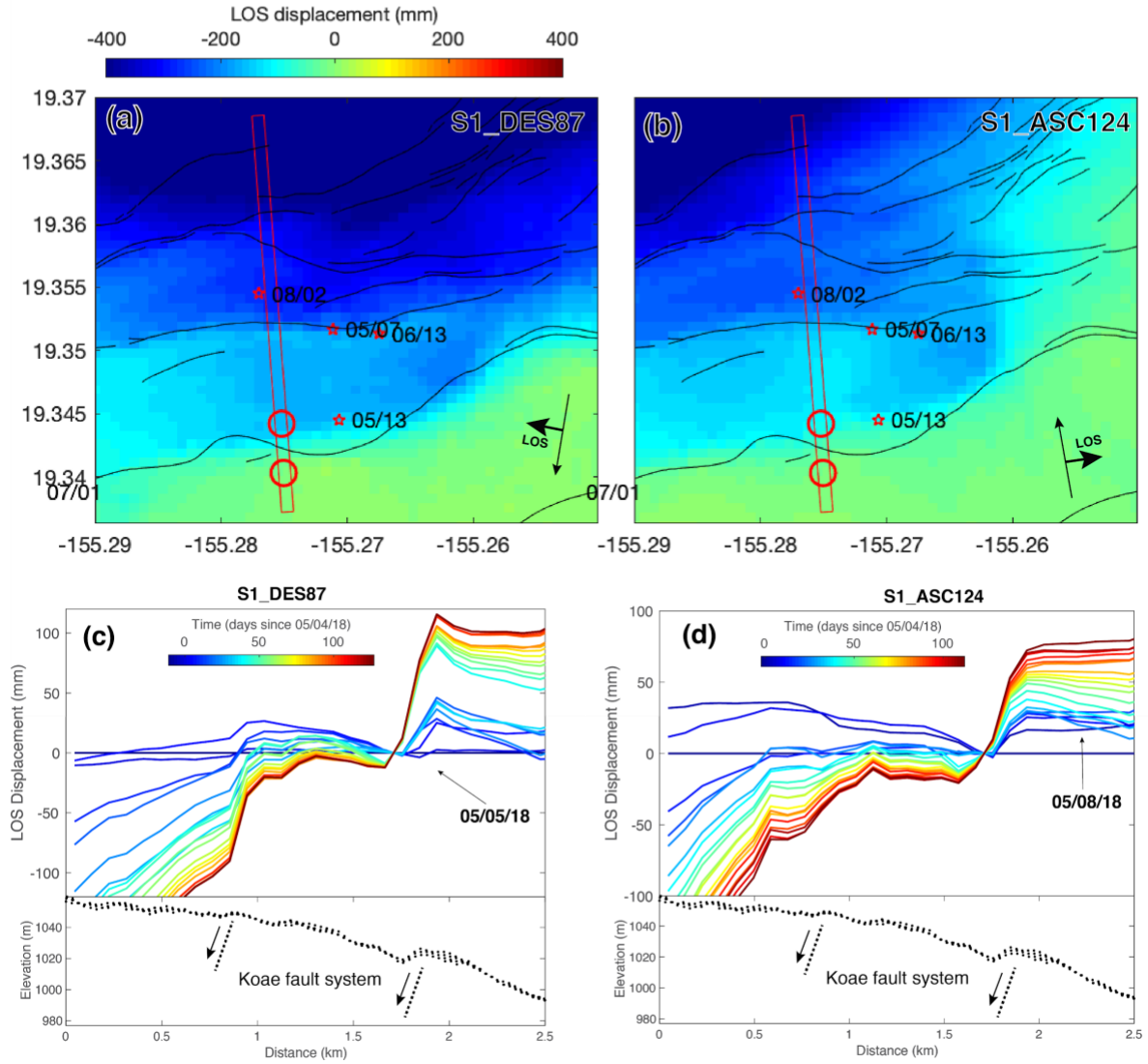


Figure S6. LOS displacements across the Koa'e fault system derived from Sentinel-1 data. (a)-(b) cumulative LOS displacements from January to November 2018 around the KFS. Red stars represent shallow (depth < 1 km) earthquakes of  $M > 3.5$  that are likely hosted by the KFS. (c)-(d) Postseismic LOS displacement time series along a profile across the KFS. Note that the cumulative LOS displacements on 05/05/18 exhibit little offset across the KFS (a), suggesting that the KFS offsets are not directly associated to the M 6.9 earthquake on 05/04/2018.



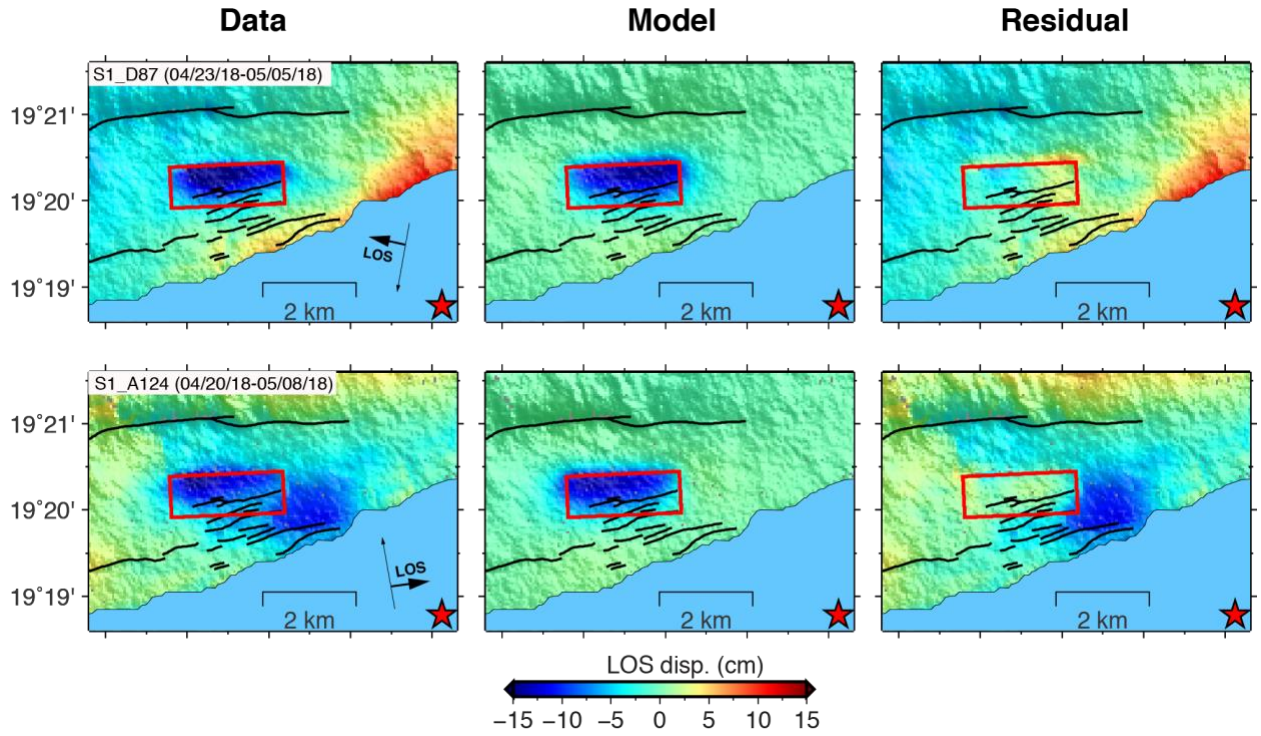


Figure S7. Comparison of observed and modeled coseismic LOS displacements due to the newly formed costal slump near the eastern end of the HFS. Red star represents the M6.9 earthquake on 05/04/2018. Red rectangular represents surface projection of the best-fitting fault patch.

Station	Longitude	Latitude	Ve (cm/yr)	Vn (cm/yr)	sigma_E(c m/yr)	sigma_N(c m/yr)
CH01	-155.1760146	19.31737127	0	-1.18	0.12	0.33
CH02	-155.175594	19.31595866	-0.08	-1.22	0.3	0.9
CH03	-155.1750157	19.31430727	-0.13	-1.08	0.15	0.15
CH04	-155.1745905	19.31326879	-0.2	-1.31	0.13	0.13
CH05	-155.1739993	19.31116392	-0.04	-1.16	0.14	0.13
CH06	-155.1731605	19.30907746	0.05	-1.19	0.18	0.17
CH07	-155.1723479	19.30724198	-0.12	-0.96	0.14	0.13
CH08	-155.1706746	19.30251674	-0.01	-0.93	0.2	0.2
CH09	-155.1683593	19.29392839	-0.25	-0.8	0.22	0.2
CH10	-155.1593144	19.31522221	-0.02	-0.66	0.18	0.36
CH11	-155.1594402	19.31439941	0.12	-0.74	0.24	0.3
CH12	-155.1589646	19.31205657	-0.07	-0.64	0.21	0.15
CH13	-155.1575852	19.30778937	0.32	-0.91	0.3	0.15
CH14	-155.1555458	19.30188926	0.2	-0.41	0.45	0.36
CH15	-155.1528667	19.29585189	-0.06	-0.71	0.12	0.78
CH16	-155.1514192	19.28983398	-0.1	-0.81	0.29	0.24
CH17	-155.151107	19.28751911	-0.05	-0.46	0.09	0.09
CH18	-155.1478846	19.27812736	0	0	0.1	0.1
HVO7710	-155.17617	19.32022	-0.38	-0.82	0.06	0.06
M801	-155.16742	19.31698	0.15	-0.83	0.09	0.36
BM79503	-155.1588509	19.31632382	0.03	-0.53	0.24	0.33
Z	-155.1471364	19.31354524	0.09	-0.21	0.15	0.15
HVO63	-155.1420229	19.31290717	0.28	-0.35	0.27	0.57
HVO64	-155.1363757	19.3139151	0.36	0.15	0.32	0.29
BM79504	-155.1413674	19.30772857	-0.02	-0.33	0.22	0.19
HVO7715	-155.1500359	19.30500614	0.21	-0.59	0.39	0.21
HVO7716	-155.1539481	19.29881996	-0.18	-0.71	0.36	0.09
HVO88-4	-155.150241	19.29655499	0.13	-0.73	0.24	0.33
HVO7717	-155.1474524	19.29297789	-0.15	-0.37	0.19	0.16
BM79505	-155.1378104	19.29162943	0.15	0.28	0.51	0.96
HVO76	-155.1312099	19.28949832	0.28	-0.05	0.16	0.15
HVO77	-155.1260936	19.28639951	0.23	0.06	0.18	0.17
HVO78	-155.1211065	19.28345972	0.17	0.31	0.21	0.21

Table S1. GPS velocity across the HFS during 2001 and 2010. All velocities are relative to the station CH18.

Station	Longitude	Latitude	Ve(cm/yr)	Vn(cm/yr)	sigma_E(cm/yr)	sigma_N(cm/yr)
CH01	-155.1760146	19.31737127	-0.64	-0.83	0.49	0.65
CH02	-155.175594	19.31595866	-0.72	-0.58	0.5	0.64
CH03	-155.1750157	19.31430727	-0.38	-0.73	0.33	0.62
CH04	-155.1745905	19.31326879	0	-0.78	0.35	0.42
CH05	-155.1739993	19.31116392	-0.64	-0.78	0.34	0.65
CH06	-155.1731605	19.30907746	-0.49	-0.58	0.64	0.38
CH07	-155.1723479	19.30724198	-0.22	-0.83	0.36	0.54
CH08	-155.1706746	19.30251674	-0.7	-0.78	0.33	0.53
CH09	-155.1683593	19.29392839	-0.38	-0.34	0.29	0.32
CH10	-155.1593144	19.31522221	-0.53	-1.09	0.33	0.27
CH11	-155.1594402	19.31439941	-0.32	-1.21	0.4	0.28
CH12	-155.1589646	19.31205657	-0.13	-1.3	0.32	0.23
CH13	-155.1575852	19.30778937	-0.46	-1.09	0.3	0.51
CH14	-155.1555458	19.30188926	-0.1	-0.95	0.33	0.32
CH15	-155.1528667	19.29585189	0.07	-0.43	0.65	0.57
CH16	-155.1514192	19.28983398	0.07	0.12	0.43	0.44
CH17	-155.151107	19.28751911	-0.05	-0.26	0.2	0.47
CH18	-155.1478846	19.27812736	0	0	0.38	0.34
HVO7710	-155.17617	19.32022	-0.53	-0.57	0.29	0.3
M801	-155.16742	19.31698	-0.71	-1.13	0.25	0.24
BM79503	-155.1588509	19.31632382	-0.31	-0.97	0.16	0.26
Z	-155.1471364	19.31354524	-0.08	-1.28	0.19	0.41
HVO63	-155.1420229	19.31290717	0.07	-1.14	0.22	0.43
HVO64	-155.1363757	19.3139151	0.28	-0.85	0.19	0.45
BM79504	-155.1413674	19.30772857	0.26	-0.73	0.24	0.35
HVO7715	-155.1500359	19.30500614	0.04	-0.78	0.21	0.28
HVO7716	-155.1539481	19.29881996	-0.11	-0.85	0.14	0.27
HVO88-4	-155.150241	19.29655499	0.26	-0.97	0.43	0.47
HVO7717	-155.1474524	19.29297789	0.26	-0.74	0.47	0.42
BM79505	-155.1378104	19.29162943	0.54	-0.37	0.37	0.54
HVO76	-155.1312099	19.28949832	0.4	-0.56	0.36	0.57
HVO77	-155.1260936	19.28639951	0.02	-0.04	0.41	0.53
HVO78	-155.1211065	19.28345972	0.32	0.7	0.41	0.47

Table S2. GPS velocity across the HFS during 2010 and 2017. All velocities are relative to the station CH18.